Int. J. Heat Mass Transfer. Vol. 31, No. 11, pp. 2251–2259, 1988
Printed in Great Britain

0017–9310/88 $3.00+0.00

Heat transfer in laminar flow through circular tubes accounting for two-dimensional wall conduction

ANTONIO CAMPO and CARLOS SCHULER
Depto. de Termodinámica, Universidad Simón Bolívar, Caracas, Venezuela

(*Received* 11 *May* 1987 *and in final form* 11 *April* 1988)

Abstract—This paper examines the influence of a finite heated length on the heat transfer characteristics of laminar flows through thick-walled circular tubes. Under the assumption of temperature-invariant properties, this kind of conjugate problem is governed by four dimensionless groups: the length of the heated region, the Peclet number, the solid–fluid thermal conductivity ratio, and the radii ratio of the solid wall. From numerical solutions via the control volume approach, it was found that the two-dimensional wall offers a heat flow path into the fluid flow controlling the parameters of interest such as, the bulk temperature of fluid and both internal and external surface temperatures of the solid wall. From a set of typical cases analysed, it was concluded that both surface temperatures exhibited a substantial variation in the axial direction and lesser and more gradual variations were exhibited for the distribution of bulk temperature. A radical limiting solution based on a one-dimensional domain approximation of the conduction equation for the wall is also explained in detail.

INTRODUCTION

HEAT TRANSFER by forced convection in internal laminar flows has been analysed extensively for a wide variety of thermal boundary conditions. A compendium of analytical and numerical solutions for the thermal entrance region of ducts has been documented in the monograph by Shah and London [1]. From an analysis of the information contained there, it is apparent that the thermal boundary conditions of uniform axial and peripheral wall temperature and uniform axial and peripheral heat rate are realized in many practical applications. For thin-walled pipes, these two conditions are equally valid for the external surface as well as for the internal surface, in other words the solid–fluid interface. However, for relatively thick-walled pipes, the boundary conditions imposed at the external surface, in general, are different from their counterparts at the internal surface. From physical reasoning, these deviations arise because the wall plays a significant role distributing the heat coming from the external surface to the fluid flow itself. Under these extreme circumstances, the thermal boundary conditions at the solid–fluid interface are no longer known *a priori*. Such interactive situations have been referred to by Luikov *et al.* [2] as conjugate problems in the heat transfer literature. Correspondingly, this kind of problem needs to be reformulated within the generalized framework of the entire solid–fluid system, wherein the temperature and heat flow at the solid–fluid interface are controlled by the conductive–convective interaction taking place there. This generalized approach considers rigorously the simultaneous effect of axial and transversal heat conduction in the tube wall of finite length. Accordingly, a combined solution incorporating both fluid and solid media has to be obtained. In view of the foregoing, Mori *et al.* [3] were the first investigators who examined the above-mentioned conjugate problem for a circular tube considering two thermal boundary conditions specified at the outer surface, i.e. uniform temperature and uniform heat flux. They assumed the temperature distribution at the wall–fluid interface in a power series form having unknown coefficients. Correspondingly, the solution of the energy equation for the fluid was obtained directly by superposing the classical Graetz solution using the temperature distribution at the interface boundary condition. Similarly, for the particular case of uniform heat flux applied at the external surface, the authors used the Graetz series outlined by Siegel *et al.* [4], wherein the first seven eigenvalues were computed. In view of this, the main advantage of the procedure employed in ref. [4] is that only one term needs to be evaluated in the region where the temperature is considered as fully developed. On the contrary, its unattractive feature is that the number of terms required in the series for good accuracy increases drastically close to the entrance of the heat exchange region.

Conversely, the solution to the conduction equation for the wall domain was derived readily. Therefore, equating both distributions of temperature and heat flux across the solid and fluid media, Mori *et al.* [3] completed the combined solution for the conjugate problem, once the unknown coefficients of the power series were evaluated.

At this stage, it should be pointed out that the

NOMENCLATURE

a	parameter, equation (1a)
h	local convective coefficient [W m^{-2} °C^{-1}]
k_f	thermal conductivity of fluid [W m^{-1} °C^{-1}]
k_s	thermal conductivity of wall [W m^{-1} °C^{-1}]
K	parameter, equation (1a)
K_{sf}	k_s/k_f
L	length of heated region [m]
L^*	dimensionless value of L, $L/r_i\,Pe$
Nu	local Nusselt number, $2hr_i/k_f$
Pe	Peclet number, $2\bar{u}r_i/\alpha_f$
q_{wi}	convective heat flux at the internal surface [W m^{-2}]
q_w	applied wall heat flux at the external surface [W m^{-2}]
r	radial coordinate [m]
r_i	internal radius of wall [m]
r_e	external radius of wall [m]
r^*	dimensionless coordinate, r/r_i
r_e^*	r_e/r_i
t	wall thickness, $r_e - r_i$ [m]
T	temperature [°C]
u	velocity of fluid [m s^{-1}]
$\bar{u}$	mean velocity of fluid [m s^{-1}]
u^*	$u/\bar{u}$
x	axial coordinate [m]
x^*	dimensionless coordinate, $x/r_i\,Pe$.

Greek symbols

α_f	thermal diffusivity of fluid [m^2 s^{-1}]
β	wall conductance parameter, equation (11)
ϕ	dimensionless temperature, $k_f(T-T_0)/q_w r_e$
Φ_w	mean temperature of the wall, equation (10)
Ω	dimensionless heat transfer rate, equation (9).

Subscripts

b	bulk
e	external surface
i	internal surface
w	wall
0	inlet.

analytical solution developed in ref. [3] may present some inaccuracies in the vicinity of the origin of the heat exchange section, and also for the entire section when its length becomes very small. This anomalous behaviour may be attributed to the fact that the analytical solution relies on the use of only seven eigenvalues as reported in ref. [4]. On the other hand, it should be added that, Luikov *et al.* [2] delineated a mathematical procedure for the above-mentioned conjugate problem, but their closed-form solution involved highly complicated functions and because of this, no numerical results were reported.

Additionally, Barozzi and Pagliarini [5] re-examined the wall conduction effect of the problem treated in ref. [3] using a numerical procedure that combines the finite-element method in the solid wall and the Duhamel theorem at the fluid–solid interface. They used the heat transfer coefficient as the vehicle for transmitting information through the interface during the required iteration process.

The main objective of the present study is to provide an alternate finite-difference procedure for the problem of laminar forced convection through thick-walled tubes exposed to a uniform heat flux in a finite length. The numerical solution relies on the control volume approach devised by Patankar [6]. A schematic diagram of the physical situation and the appropriate coordinate system is shown in Fig. 1. A search of the open literature failed to disclose any prior work on the solution method outlined in the preceding paragraphs to the problem under study here, except the publications of Mori *et al.* [3] and Barozzi and Pagliarini [5]. In this study, the numerical procedure was based on an iterative scheme which dealt simultaneously with the fluid and the wall domains. The computed results depend on four controlling parameters: the Peclet number, the fluid–solid conductivity ratio, the wall thickness and the finite length of the heated region. In presenting these results, account was taken of the important fact that the only relevant quantities of interest for practical problems are the local bulk temperature of the fluid and the local internal and external surface temperatures of the wall, all unknown functions of the axial coordinate. Consequently, numerical results are presented for each of these quantities, expressed in suitable dimensionless forms. In addition to this, some local Nusselt numbers are computed also for selected cases and they are presented for purposes of comparison only.

The computational procedure employed in this paper is being extended to other more complex situ-

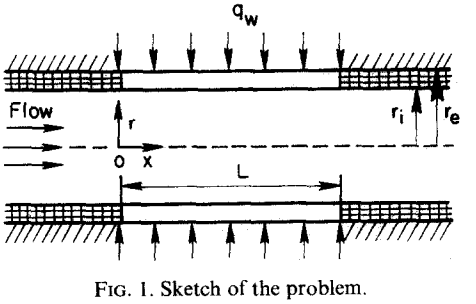

FIG. 1. Sketch of the problem.

ations involving combined mechanisms of heat transfer that do not admit closed-form solutions.

There is, of course, related work which forms some background for the wall conduction effects that were investigated here [7–10]. However, they differ from the main lines of the present research.

STATEMENT OF THE PROBLEM

In this paper, the physical model under consideration consists of a constant property fluid flowing laminarly through a circular tube as shown in Fig. 1. At the entrance of the finite heat exchange region, the velocity is assumed fully developed, while the temperature is taken as uniform. The heating takes the form of a uniform axial and peripheral heat flux imposed at the outside surface of the tube. As noted earlier, consideration is being given here to relatively thick walls so that temperature variations along the wall and across its thickness are important. Hence, in view of this, the influence of the wall thickness of the tube in the thermal development region involves the application of a two-dimensional energy equation for both the fluid and solid regions. These governing equations are expressed in compact form as follows:

$$\frac{u^*}{2}\frac{\partial\phi}{\partial x^*} = \frac{1}{r^*}\frac{\partial}{\partial r^*}\left(r^* K \frac{\partial\phi}{\partial r^*}\right) + \frac{aK}{Pe^2}\frac{\partial^2\phi}{\partial x^{*2}} \quad (1a)$$

where, for the fluid domain $(0 < r^* < 1)$

$$u^* = 2(1-r^{*2})$$
$$K = 1$$
$$a = 0 \quad (1b)$$

and, for the solid domain $(1 < r^* < r_e^*)$

$$u^* = 0$$
$$K = K_{sf}$$
$$a = 1. \quad (1c)$$

The relevant boundary conditions associated with this highly coupled conjugate heat transfer problem are

$$\phi = 0, \qquad x^* = 0,\ 0 < r^* < 1 \quad (2a)$$

$$\frac{\partial\phi}{\partial x^*} = 0, \qquad x^* = 0,\ 1 < r^* < r_e^* \quad (2b)$$

$$\frac{\partial\phi}{\partial r^*} = 0, \qquad r^* = 0,\ 0 < x^* < L^* \quad (2c)$$

$$r_e^* K_{sf}\frac{\partial\phi}{\partial r^*} = 1, \qquad r^* = r_e^*,\ 0 < x^* < L^* \quad (2d)$$

$$\frac{\partial\phi}{\partial x^*} = 0, \qquad 1 < r^* < r_e^*,\ x^* = L^*. \quad (2e)$$

In the preceding equations, the dimensionless variables are defined by

$$\phi = \frac{T-T_0}{q_w r_e/k_f}, \quad r^* = \frac{r}{r_i}$$
$$x^* = \frac{x}{r_i\, Pe}, \quad L^* = \frac{L}{r_i\, Pe} \quad (3)$$

while the remaining symbols are described in the Nomenclature.

Solution of the set of equations (1)–(3) by numerical techniques provides the two-dimensional temperature fields for the fluid and the solid under the influence of a uniform wall heat flux applied at a finite length. This detailed information was processed and eventually employed to evaluate various thermal quantities of interest for inclusion in the presentation of results. One of these quantities is the local mean bulk temperature of the fluid, which in dimensionless form, can be expressed as

$$\phi_b(x^*) = 2\int_0^1 u^*\phi r^*\,dr^*. \quad (4)$$

It should be noted that calculation of this global quantity is mandatory because the linear bulk temperature rise which is characteristic of uniform heated flows confined by inactive walls does not prevail here.

In addition to the mean bulk temperature, other quantities of interest are the variations of the internal and external surface temperatures ϕ_{wi} and ϕ_{we} with x^*. Numerical evaluation of these quantities will be reported later and are obtained directly from the temperature fields.

On the other hand, the local Nusselt number distribution may be evaluated from its conventional definition

$$Nu = \frac{-2q_{wi}^*}{\phi_b(x^*)-\phi_{wi}(x^*)} \quad (5)$$

where q_{wi}^* designates the dimensionless heat flux across the internal surface of the tube given by

$$q_{wi}^* = \left.\frac{\partial\phi}{\partial r^*}\right|_{r^*=1^{(-)}}. \quad (6)$$

In this equation, the superscript $(-)$ means that the derivative has been numerically evaluated at the fluid side of the solid–fluid interface.

Conversely, at this stage, it should be emphasized that calculation of the local Nusselt number has been performed with the sole purpose of validating the methodology and comparing our results against others published in the literature. Nevertheless, the total heat transferred to the fluid flow may be easily determined from an energy balance between the stations $x = 0$ and L. This energy balance serves to relate the dimensionless bulk temperature ϕ_b to a so-called heat transfer efficiency, defined as

$$\Omega = Q_{T\,fluid}/Q_{input}. \quad (7)$$

In this equation, Q_{input} denotes the amount of heat

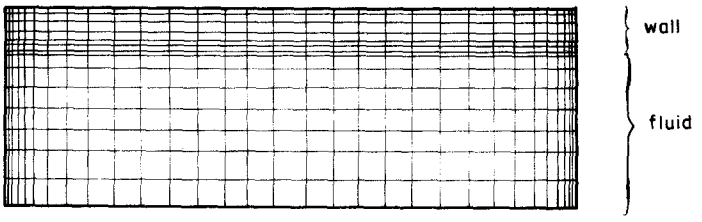

FIG. 2. Computational domains.

transfer applied at the external surface of the tube wall. In light of the foregoing

$$Q_{\text{T fluid}} = \dot{m}c_p[T_b(L) - T_0]. \tag{8a}$$

Upon introducing the dimensionless temperature ϕ, equation (8a) becomes

$$Q_{\text{T fluid}} = \rho c_p \bar{u}\pi r_i^2 \frac{q_w r_e}{k_f}\phi_b. \tag{8b}$$

Therefore, combining equations (7) and (8b), and rearranging terms, yields the simple relation

$$\Omega = \frac{\phi_b}{4x^*}. \tag{9}$$

The reader should note that equation (9) allows for a direct calculation of the total heat transfer rate to the fluid once the mean bulk temperature is known at $x = L$. It should be added that the conventional way to compute the heat transferred to the fluid, via the local Nusselt number, is much more elaborate requiring knowledge of the distributions of q^*_{wi}, ϕ_b and ϕ_{wi}, respectively (see equation (5)). In addition to this, the proposed approach involving equation (9) saves some space because the collection of curves for Nu is not necessary.

SOLUTION PROCEDURE

Solutions of the problem defined by the foregoing system of equations were obtained numerically using a finite-difference methodology. The difference scheme employed here for solving the energy equations for both the fluid and the solid regions is an adaptation of the control-volume approach developed by Patankar [6]. Firstly, in the fluid region, the difference equations were written under the assumption of a high Peclet number flow, wherein the axial conduction term was omitted and the convection term was evaluated on an upwind basis. To handle the abrupt change in thermal conductivity at the internal interface, a special formulation proposed by Patankar [6] is utilized. This particular formulation is based on the steady, no-source, one-dimensional situation in which the thermal conductivity varies in a stepwise fashion. To cope with enhanced accuracy, refinement of the mesh is mandatory and the grid points were positioned non-uniformly in both the fluid and the solid domains. Accordingly, in the radial direction, the grid point density was highest in the neighbourhood of the interface, whereas in the axial direction the highest concentration of grid points was placed in the vicinity of $x^* = 0$ and L^*, respectively, as shown in detail in Fig. 2. Moreover, the grid deployment in the radial direction was plotted according to a suitable stretching transformation from a family of general stretching transformations proposed by Roberts [11].

On the other hand, it should be added that the salient feature of the numerical methodology employed in this study is that the resulting penta-diagonal system of algebraic equations was solved by implementing the MSI algorithm developed by Schneider and Zedan [12]. Among the advantages provided by this powerful algorithm, it can be said that it is between two and four times faster than the traditional algorithms commonly used for this kind of system in the literature.

Changing the attention to the grid employed in this paper, a total of 900 grid points were used in the fluid–solid domain. A total of 20 and 10 grid points were deployed in the fluid and the solid regions, respectively, at each of 30 axial stations. Furthermore, comparisons were made with the solution using 10 points in the fluid and 5 points in the solid showing that convergence was met within plotting accuracy.

Accuracy tests of the computational scheme proposed here were made by comparison with the limiting condition of uniform heat flux with a non-participating wall, reported by Shah and London [1]. In addition to this, comparison was also made with the analytical solution presented by Mori *et al.* [3] for the problem described above, but with a two-dimensional participating wall. The latter authors based their solution on seven eigenvalues reported in ref. [4]. In general, agreement was very good for both situations having passive and active walls.

ONE-DIMENSIONAL MODEL

Attention will now be focused on the energy equation for the tube wall. As noted earlier, consideration is being given in this study to finite thick walls so that temperature variations along and across the wall cannot be neglected.

Let us consider the idealization that only one nodal point is deployed in the wall region, so that the present methodology reduces to the widely known one-dimensional approximation. This formulation assumes that temperature changes across the thickness of the wall are relatively small, and accordingly the wall mean

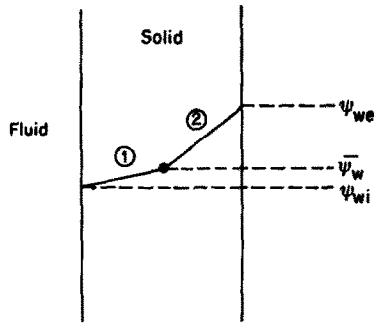

① Slope obtained from the temperature gradient in the fluid

② Slope obtained from the value of q_w

FIG. 3. Sketch for the coupling between the temperature distributions.

temperature distribution Ψ_w is governed by the dimensionless ordinary differential equation

$$\frac{\beta}{Pe^2}\frac{d^2\Psi_w}{dx^{*2}} + 1 - q^*_{wi} = 0 \qquad (10)$$

where q^*_{wi} is the dimensionless heat flux distribution at the internal surface. The energy balance that leads to equation (10) incorporates some differences between the analysis developed by Faghri and Sparrow [7] and the present analysis. They will be explained in detail in the following paragraphs.

First, the wall conductance parameter β accounts for the magnitude of the wall curvature, which is normally omitted in the conventional one-dimensional model. In view of this, β, when written explicitly, has the form

$$\beta = K_{sf}\frac{t}{r_i}\left(\frac{t}{2r_i}+1\right) \qquad (11)$$

where $t = r_e - r_i$ is the wall thickness. The term in parentheses on the right-hand side of equation (11) gives full account of the effect of the tube curvature. This quantity becomes negligible whenever the analysis is restricted to thin walls (small t) and/or large diameter tubes (large r_i).

Second, the coupling between the temperature fields of the fluid and the solid is carried out via the heat flux at the interface, namely q^*_{wi} and also by using the matching condition

$$\Psi_{wi} = \bar{\Psi}_w - \frac{(r^*_e+1)}{2}\frac{q^*_{wi}}{K_{sf}} \quad \text{at any } x^*. \qquad (12)$$

Thus, based on the sketch of Fig. 3, a distinction is made between the mean temperature of the wall $\bar{\Psi}_w$ and the corresponding interface temperature Ψ_{wi} of it. This can be done by exploiting the existence of a linear temperature profile in the transversal direction of the wall. By applying the limits $r^*_e \to 1$ and $K_{sf} \to \infty$, the matching condition of equation (12) reduces to the one suggested by Faghri and Sparrow [7], namely

$$\Psi_{wi} = \bar{\Psi}_w \quad \text{at any } x^*.$$

Following the above-mentioned ideas, the temperature distribution of the external surface may be readily computed from the relation

$$\Psi_{we} = \bar{\Psi}_w + \frac{(r^*_e+1)}{2}\frac{1}{2K_{sf}r^*_e}. \qquad (13)$$

RESULTS AND DISCUSSION

From an engineering point of view, it is not convenient to present numerical results for this convective–conductive conjugate problem in terms of the conventional Nusselt numbers or the equivalent heat transfer coefficients. The reason for this statement is that, for this kind of conjugate problem, computation of the heat transfer coefficient involves three unknown quantities, namely: q^*_{wi}, ϕ_{wi} and ϕ_b, all functions of x^*, as stated in equation (5). Consequently, by specifying the variation of Nu in the axial direction, there is no possible way to evaluate the heat transfer characteristics of the fluid flow for practical applications. Seemingly, this fact was not realized by Mori *et al.* [3], who presented their results in terms of Nu and ϕ_{wi} only; q^*_{wi} and ϕ_b remaining as unknown quantities not reported in the paper. In view of this limitation, their graphical results are of little applicability for calculation of engineering problems, other than to establish that the Nu distributions are bounded by the corresponding distributions for uniform wall temperature and uniform wall heat flux involving thermally inactive walls, respectively. Conversely, in the present work, we proposed a totally different approach, wherein results will be presented in terms of realistic thermal parameters, namely: the distributions of bulk temperature ϕ_b and local temperatures ϕ_{wi} and ϕ_{we} accounting for two-dimensional wall conduction. All of these local variables are of paramount interest in engineering applications.

A detailed inspection of the governing system of equations (1)–(3), reveals that the temperature distributions of the fluid and the solid are dependent on four parameters, namely: Pe, K_{sf}, r^*_e and L^*. In recognition of this excessive number of parameters, numerical solutions were obtained for two Peclet numbers ($Pe = 500$ and 1500) and two representative values of the radii ratio r^*_e encountered in practical problems, such as $r^*_e = 1.02$ and 1.2, with a range of conductivity ratio K_{sf} for each combination of Pe and r^*_e ranging from $K_{sf} = 1$ to a maximum of $K_{sf} = 10^4$. All calculations correspond to a fixed heated length, $L^* = 0.04$ used in ref. [3] too. Due to space limitations, a representative sample involving combinations of this set of parameters only is presented in this section.

At this juncture, it should be pointed out that the choice of the external radius r_e instead of the internal

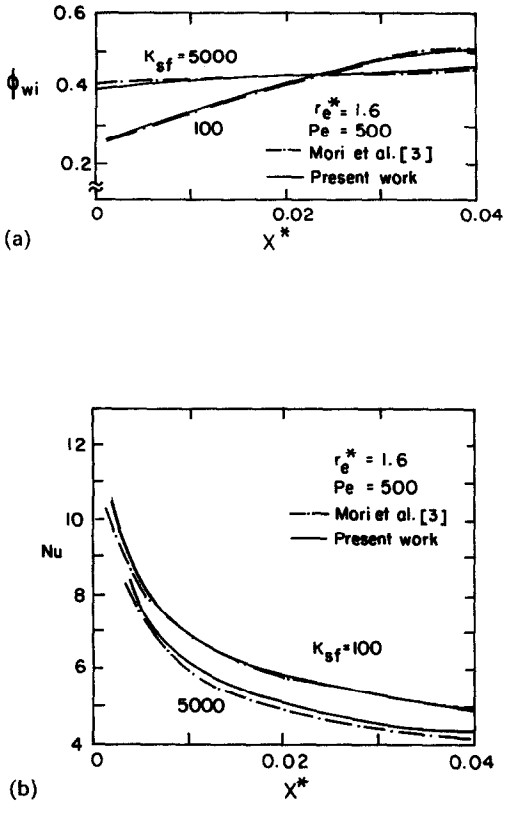

FIG. 4. Comparison for the distributions of internal surface temperature and Nusselt number.

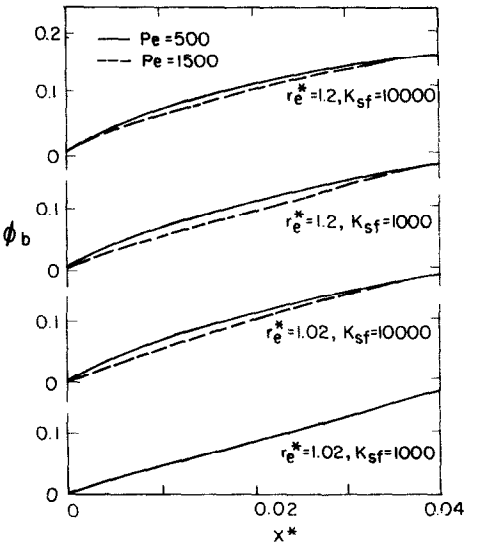

FIG. 5. Distributions of mean bulk temperature.

radius r_i as the characteristic length in the definition of the dimensionless temperature ϕ appearing in equation (3), ensures that the total amount of heat applied at the external surface of the tube wall is independent of the value of the radii ratio r_e^*. Thus, in view of this, computed results are compatible in the whole range of cases analysed here, because the same amount of heat is supplied to the fluid stream always. It should be emphasized that this definition has been employed by Mori *et al.* [3] also, but it differs from the one used by Faghri and Sparrow [7], who neglected the wall curvature of the tube.

Firstly, to assess the validity of the present numerical methodology, a typical set of results in terms of the distributions of internal surface temperature and local Nusselt number are depicted in Figs. 4(a) and (b), respectively. These variables were chosen in ref. [3] to report their numerical results. The corresponding family of curves is plotted for $r_e^* = 1.6$, $Pe = 500$ and $K_{sf} = 100$ and 5000. As observed in the figures, agreement was found to be excellent in the entire heating region of the tube.

As mentioned in the preceding paragraphs, results will be presented for the axial distributions of three quantities: the mean bulk temperature ϕ_b, the internal surface temperature ϕ_{wi} and the external surface temperature ϕ_{we}. The general trends of these results will be discussed in the following paragraphs.

Axial distribution of the mean bulk temperature between $x^* = 0$ and 0.04 is presented in Fig. 5. The major issue to be examined in this figure is the response of ϕ_b to the variations of the controlling parameters r_e^*, K_{sf} and Pe. Examination of the curves of Fig. 5 reveals that for the set of parameters chosen, the mean bulk temperatures at the exit of the heating region, i.e. $x^* = 0.04$ are essentially identical. Meanwhile, for a fixed value of r_e^*, the effect of the conductivity ratio K_{sf} is to increase slightly the bulk temperature at intermediate stations, and at the final stations too. This outcome is especially noteworthy since the mean bulk temperature is one of the most important quantities that needs to be computed as a result of heat addition at the external surface of the tube (finite length), with respect to the case of thermally inactive walls (infinite length). In addition to this, the influence of the Peclet number ($Pe = 500$, 1500) for each group of curves is not relevant at all.

An even more convincing demonstration of the forgiving nature of temperature to small values of K_{sf} may be seen by examining Fig. 6, which was drawn for $r_e^* = 1.02$. Here, it is observed that for K_{sf} up to 100, the distributions of internal surface temperature are almost identical and independent of Pe. However, for a moderate value of $K_{sf} = 1000$, the corresponding curve shows a drastic distortion in the vicinity of both $x^* = 0$ and 0.04, when compared to the ones already discussed. For $Pe = 500$, the temperature at $x^* = 0$ is increased two-fold, whereas the temperature at $x^* = 0.04$ has been reduced by a small percentage only. This trend is slightly modified for the case characterized by $Pe = 1500$. The last curve plotted in Fig. 6 corresponds to the case of $K_{sf} = 10\,000$. Here again, the internal surface temperature tends to level off. Moreover, for a fixed $Pe = 500$, the temperature at $x^* = 0$ increases by a factor of three, while its value at the exit $x^* = 0.04$ experiences a reduction of

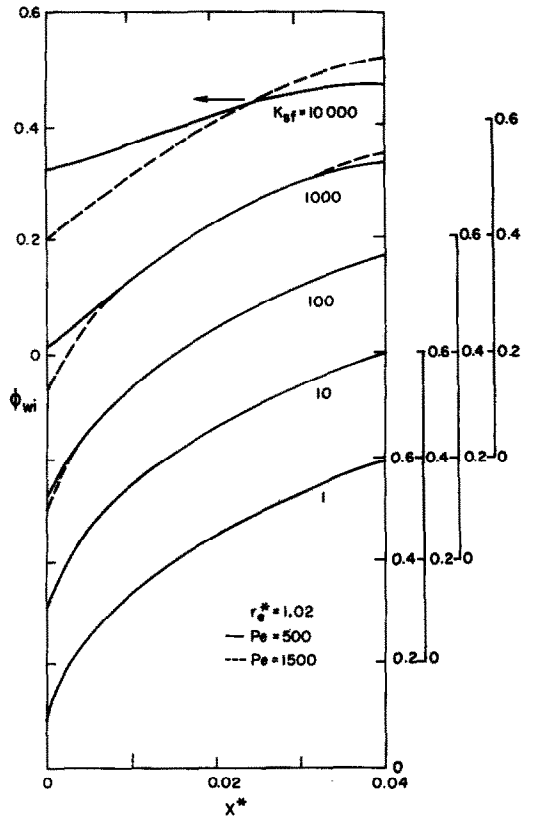

FIG. 6. Distributions of internal surface temperature.

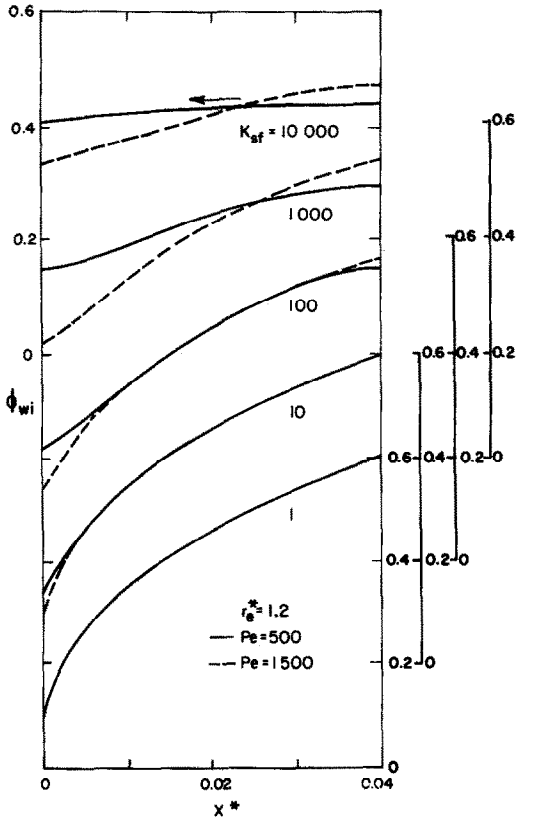

FIG. 7. Distributions of internal surface temperature.

approximately 10%. The distortion of the corresponding curve for $Pe = 1500$ is not as pronounced.

Attention is now turned to the same situation examined in Fig. 5, but increasing the radii ratio r_c^* to 1.2. Thus, Fig. 7 has been prepared for this purpose. The curves for $K_{sf} = 1$ and 10 remain unaltered, while the distribution changes gradually at both ends of the heating region beginning now with $K_{sf} = 100$. The internal surface temperature at $x^* = 0$ associated with $K_{sf} = 1000$ increases significantly, while its value at $x^* = 0.04$ drops slightly. This pattern is even more pronounced for $K_{sf} = 10^4$, where the interfacial temperature becomes almost uniform for $Pe = 500$. This conclusion may be drawn from Fig. 5 too, if a curve for a higher value of K_{sf}, say $K_{sf} = 10^5$, is available.

At this point, it is interesting to note in Figs. 6 and 7 that, regardless of the numerical values of r_c^* and Pe, the internal surface temperature always reaches an asymptotic uniform value (average value) $\Psi_{w\infty}$ as $K_{sf} \to \infty$ for a fixed heating length $L^* = 0.04$. In the particular case of Fig. 7, $\Psi_{wi} = 0.43$ approximately, while Ψ_{wi} is slightly less in Fig. 6, both based on $K_{sf} = 10\,000$. This preliminary analysis suggests that $\Psi_{w\infty}$ is independent of r_c^* and Pe and depends exclusively on L^*. Therefore, under these extreme circumstances, let us assume the existence of an interfacial temperature $\Psi_{w\infty}$ that is axially uniform. Accordingly, performing a global energy balance between the entrance $x^* = 0$ and the exit of the heating region $x^* = L^*$, results in the simple expression

$$\Psi_{w\infty} = \frac{4L^*}{[1 - t_b(L^*)]}. \tag{14}$$

In this equation t_b designates the dimensionless bulk temperature under the idealization of uniform wall temperature and inactive walls, i.e. the so-called classical Graetz problem. In this sense, an accurate calculation of the corresponding bulk temperature distribution has been performed by Shah [13] and is reported in ref. [1].

In order to test the validity of equation (14), let us carry out a simple computation. Since in this study $L^* = 0.04$, the value of t_b at this axial station, taken from ref. [13] is $t_b = 0.628$. Inserting these two numbers into equation (14) yields $\Psi_{w\infty} = 0.43$. This value coincides with the reading of ϕ_{wi} for $K_{sf} = 10\,000$ in Fig. 7. Similarly, this trend is also manifested in Fig. 6, although the isothermal limit is achieved at a higher value of K_{sf}.

A comparison between the internal and external temperature distributions for $r_c^* = 1.2$, $Pe = 500$ and $K_{sf} \geqslant 1$ is depicted in Fig. 8. For this particular combination, it is observed that the Ψ_{wi} and Ψ_{we} curves for $K_{sf} = 1$ are quite far apart, but whenever $K_{sf} \geqslant 10$ deviations between these two temperatures are unnoticed. This negligible difference prevails always for high values of K_{sf} and small values of r_c^*. This

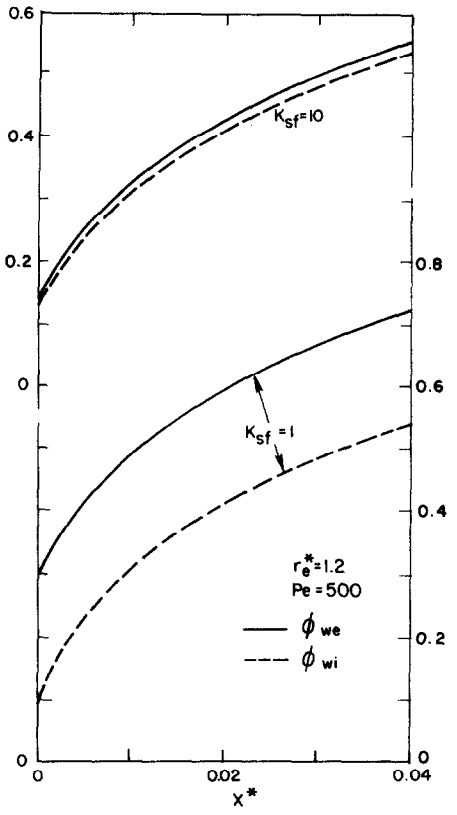

FIG. 8. Distributions of internal and external surface temperatures.

peculiar behaviour suggests that, under the circumstances delineated above, the one-dimensional approximation may be valid, and consequently simplifies the analysis of the conjugate problem drastically.

Ultimately, Fig. 9 has been prepared to compare the results of the interfacial temperature distribution based on the one- and two-dimensional models proposed here, and additionally to assess the sensitivity of the one-dimensional results. In view of the large

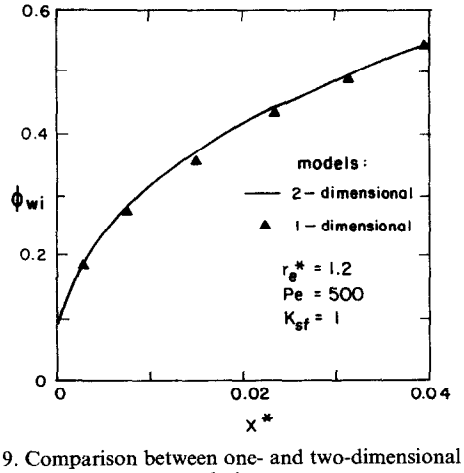

FIG. 9. Comparison between one- and two-dimensional formulations.

number of parameters involved, a rather critical case having $r_e^* = 1.2$, $Pe = 500$ and the smallest possible value of K_{sf}, $K_{sf} = 1$ was selected for testing purposes. An overall inspection of the figure reveals that there is no substantial difference in the interfacial temperature yielded by the one- and two-dimensional models. It should be added that computations based on the two-dimensional model utilized ten radial nodes in the wall domain.

As a final remark, a few comments on the efficiency of the computational procedure are in order. As already noted, the finite-difference grid for the forced convection domain consisted of 30×30 points (axial $\times$ radial). Meanwhile, the grid for the conduction problem in the solid was made of 30×10 points (axial $\times$ radial), the circumferential distribution of which matched that for the forced convection domain. The computation time was surprisingly small. A typical run took approximately 15 s of CPU time to achieve convergence of up to four decimal figures on a DEC-10 digital computer. In passing, it should be added that the computational scheme developed in this paper shows high numerical stability; e.g. solutions using a coarse grid consisting of four radial nodes in the fluid and only one node in the solid agree well with those utilizing more refined grids.

REFERENCES

1. R. K. Shah and A. L. London, *Laminar Flow Forced Convection in Ducts*. Academic Press, New York (1978).
2. A. V. Luikov, V. A. Aleksashenko and A. A. Aleksashenko, Analytical methods of solution of conjugated problems in convective heat transfer, *Int. J. Heat Mass Transfer* **14**, 1047–1056 (1971).
3. S. Mori, M. Sakakibara and A. Tanimoto, Steady heat transfer to laminar flow in a circular tube with conduction in the tube wall, *Heat Transfer—Jap. Res.* **3**(2), 37–46 (1974).
4. R. Siegel, E. M. Sparrow and T. M. Hallman, Steady laminar heat transfer in a circular tube with prescribed wall heat flux, *Appl. Scient. Res.* **A7**, 386–392 (1958).
5. G. S. Barozzi and G. Pagliarini, A method to solve conjugate heat transfer problems: the case of fully developed laminar flow in a pipe, *J. Heat Transfer* **107**, 77–83 (1985).
6. S. V. Patankar, *Numerical Heat Transfer and Fluid Flow*. McGraw-Hill, New York (1980).
7. M. Faghri and E. M. Sparrow, Simultaneous wall and fluid axial conduction in laminar pipe-flow heat transfer, *J. Heat Transfer* **102**, 58–63 (1980).
8. A. Campo and R. Rangel, Lumped-system analysis for the simultaneous wall and fluid axial conduction in laminar pipe-flow heat transfer, *PhysicoChem. Hydrodyn.* **4**, 163–173 (1983).
9. E. K. Zariffeh, H. M. Soliman and A. C. Trupp, The combined effects of wall and fluid axial conduction on laminar heat transfer in circular tubes, *Heat Transfer 1982* **4**, 131–135 (1982).
10. N. E. Wijeysundera, Laminar forced convection in circular and flat ducts with wall axial conduction and external convection, *Int. J. Heat Mass Transfer* **29**, 797–807 (1986).
11. G. O. Roberts, Computational meshes for boundary

layer problems. In *Lecture Notes on Physics*, Vol. 8, pp. 171–177. Springer, New York (1971).
12. G. E. Schneider and M. Zedan, A modified strongly implicit procedure for the numerical solution of field problems, *Numer. Heat Transfer* **4**, 1–19 (1981).
13. R. K. Shah, Thermal entry length solutions for the circular tube and parallel plates, Paper No. HMT-11-75, National Heat Mass Transfer Conference, Bombay, India (1975).

TRANSFERT THERMIQUE PAR UN ECOULEMENT LAMINAIRE DANS DES TUBES CIRCULAIRES, AVEC CONDUCTION PARIETALE BIDIMENSIONNELLE

Résumé—On examine l'influence d'une longueur finie de chauffage sur les caractéristiques du transfert thermique par des écoulements laminaires à travers des tubes circulaires à paroi épaisse. Supposant des propriétés indépendantes de la température, ce problème conjugué est gouverné par quatre groupes adimensionnels: la longueur de la région chauffée, le nombre de Peclet, le rapport des conductivités thermiques solide–fluide et le rapport des rayons sur la paroi solide. A partir des solutions numériques obtenues par la méthode du volume de contrôle, on trouve que la paroi bidimensionnelle provoque un domaine de chauffage dans le fluide qui contrôle les paramètres tels que la température moyenne du fluide et les températures des surfaces interne et externe de la paroi solide. A partir d'un ensemble de cas typiques analysés, on conclut que les deux températures de surface varient de façon sensible dans la direction axiale tandis que les variations de la température moyenne sont moindres et plus graduelles. On explique en détail une solution radicale limite basée sur une approximation monodimensionnelle de l'équation de conduction dans la paroi.

DER WÄRMEÜBERGANG BEI LAMINARER STRÖMUNG IN KREISFÖRMIGEN ROHREN MIT BERÜCKSICHTIGUNG DER ZWEIDIMENSIONALEN WÄRMELEITUNG IN DER WAND

Zusammenfassung—In diesem Bericht wird der Einfluß einer endlichen beheizten Länge auf den Wärmeübergang bei laminarer Strömung in dickwandigen kreisförmigen Rohren untersucht. Unter der Annahme von temperaturunabhängigen Stoffwerten wird dieses gekoppelte Problem von vier dimensionslosen Größen beeinflußt: der Länge der beheizten Zone, der Peclet-Zahl, dem Verhältnis der Wärmeleitfähigkeiten des Rohrs und des Fluids sowie des Radiusverhältnisses des Rohrs. Durch numerische Lösungen mit Hilfe der Kontrollvolumennäherung wurde festgestellt, daß die Längswärmeleitung in der Wand einen Einfluß auf die Temperatur des Fluids und die Wandaußen- und -innentemperatur des Rohrs hat. Aus der Betrachtung von typischen Fällen wird geschlossen, daß die beiden Oberflächentemperaturen eine wesentliche Änderung in axialer Richtung zeigen, während bei der Verteilung der Fluidtemperatur eine geringere Veränderung auftritt. Auf eine Grenzlösung, die auf einer bereichsweise eindimensionalen Näherung der Wärmeleitungsgleichung für die Wand beruht, wird ebenfalls eingegangen.

ТЕПЛОПЕРЕНОС ПРИ ЛАМИНАРНОМ ТЕЧЕНИИ В КРУГЛЫХ ТРУБАХ С УЧЕТОМ ДВУХМЕРНОЙ ТЕПЛОПРОВОДНОСТИ СТЕНКИ

Аннотация—Рассматривается влияние нагреваемого участка конечной длины на характеристики теплообмена при ламинарном течении в круглых трубах с толстой стенкой. В предположении независимости свойств от температуры для данной сопряженной задачи в качестве определяющих критериев рассматриваются: длина нагреваемого участка, число Пекле, отношение теплопроводностей твердого тела и жидкости, а также отношение радиуса трубы к толщине твердой стенки. В результате численных расчетов с использованием метода контрольного объема установлено, что изменяя условия теплоотдачи от стенки в поток жидкости, можно управлять такими важными параметрами, как среднемассовая температура жидкости, а также внутренняя и внешняя температуры поверхности твердой стенки. Анализ ряда типичных случаев показывает, что обе температуры поверхностей трубы могут существенно изменяться в осевом направлении, в то время как среднемассовая температура изменяется менее значительно и более плавно. Также детально обсуждается асимптотическое решение, базирующееся на одномерной аппроксимации теплоотдачи через стенку.